

Optimizing Area Under the Curve Measures via Matrix Factorization for Drug-Target Interaction Prediction

Bin Liu^{1*} and Grigorios Tsoumakas¹

¹ School of Informatics, Aristotle University of Thessaloniki, Thessaloniki 54124, Greece
{binliu, greg}@csd.auth.gr

Abstract

In drug discovery, identifying drug-target interactions (DTIs) via experimental approaches is a tedious and expensive procedure. Computational methods efficiently predict DTIs and recommend a small part of potential interacting pairs for further experimental confirmation, accelerating the drug discovery process. Area under the precision-recall curve (AUPR) that emphasizes the accuracy of top-ranked pairs and area under the receiver operating characteristic curve (AUC) that heavily punishes the existence of low ranked interacting pairs are two widely used evaluation metrics in the DTI prediction task. However, the two metrics are seldom considered as losses within existing DTI prediction methods. This paper proposes two matrix factorization methods that optimize AUPR and AUC, respectively. The two methods utilize graph regularization to ensure the local invariance of training drugs and targets in the latent feature space, and leverage the optimal decay coefficient to infer more reliable latent features of new drugs and targets. Experimental results over four updated benchmark datasets containing more recently verified interactions show the superiority of the proposed methods in terms of the corresponding evaluation metric they optimize.

1 Introduction

Identifying drug-target interactions (DTIs) is a key step for the drug discovery process [Ezzat *et al.*, 2018]. However, the verification of DTIs via *in vitro* experiments is still costly and time-consuming. Computational approaches, which predict the affinities of drug-target pairs, reduce the number of candidate interactions for further experimental validation, and therefore expedite the drug discovery procedure. Matrix Factorization (MF) [Ezzat *et al.*, 2017], nearest neighbors [Liu *et al.*, 2020], bipartite graph learning [Airola and Pahikkala, 2018], and deep learning [Gao *et al.*, 2018] are prevalent computational DTI prediction methods.

Area under the precision recall curve (AUPR) and area under the receiver operating characteristic curve (AUC) are two crucial threshold-independent evaluation metrics in DTI prediction [Schrynemackers *et al.*, 2013], where the threshold for whether to biologically validate a drug-target pair or not is decided by medicinal experts. AUPR severely penalizes highly ranked non-interacting pairs [Davis and Goadrich, 2006], encouraging the top part of the prediction list to contain more interacting pairs, which is crucial to the efficiency of further *in vitro* experiments. On the other hand, AUC that emphasizes minimizing the number of lower ranked interacting pairs is also important for DTI prediction, because the low ranked pairs are usually excluded from experimental verification, which leads to undiscovered drugs and drug side-effects [Pliakos and Vens, 2020].

Due to the importance of AUPR and AUC, optimizing these two metrics is expected to lead to better DTI prediction performance. Although a few methods directly optimizing AUC (or ranking loss) do exist, they only work for limited settings, such as predicting interactions between candidate drugs and a specific target [Golkov *et al.*, 2020] or a fixed set of targets [Peska *et al.*, 2017]. However, important practical applications, such as drug repositioning, require identifying the interactions of existing drugs with novel targets [Chen *et al.*, 2018]. In addition, to the best of our knowledge, there is no DTI prediction method for optimizing AUPR.

MF, initially designed for recommendation systems, has been successfully applied to DTI prediction. Nevertheless, the square loss [Zheng *et al.*, 2013] and logistic loss [Liu *et al.*, 2016] are mostly used in existing MF methods for DTI prediction. There are two MF approaches for the recommendation task that optimize user-based area under the curve metrics [Shi *et al.*, 2012; Dhanjal *et al.*, 2015]. However, they cannot be applied to DTI prediction, because they fail to handle the cold start issue present in DTI prediction [Pahikkala *et al.*, 2015] and their user-based metrics are unable to fully capture the information of the interaction matrix.

This paper derives two drug-target pair based surrogate AUPR and AUC losses, upon which two MF models for DTI prediction, namely MFAUPR and MFAUC, that optimize AUPR and AUC respectively are proposed. Both of them retain the local invariance of drugs and targets in the latent feature space via graph regularization. In addition, the optimal decay coefficient determined within a faster selection pro-

*Contact Author

cess is utilized to infer reliable latent features of novel drugs and targets involved in the test pairs. Extensive experiments demonstrate the effectiveness of MFAUPR and MFAUC.

2 Our Approaches

2.1 DTI Prediction Problem

We firstly define the DTI prediction problem, where input information are the drug and target similarities. Let $D = \{d_i\}_{i=1}^n$ be a set of drugs and $T = \{t_j\}_{j=1}^m$ be a set of target, where n and m are the number of drugs and targets, respectively. The training set for D and T consists of a drug similarity matrix $\mathbf{S}^d \in \mathbb{R}^{n \times n}$, a target similarity matrix $\mathbf{S}^t \in \mathbb{R}^{m \times m}$ and an interaction matrix $\mathbf{Y} \in \{0, 1\}^{n \times m}$, where $Y_{ij} = 1$ denotes d_i and t_j interact with each other, and $Y_{ij} = 0$ otherwise. Let (d_x, t_z) be a test pair, $\mathbf{s}_x^d \in \mathbb{R}^n$ be the similarities between d_x and D , and $\mathbf{s}_z^t \in \mathbb{R}^m$ be the similarities between t_z and T . A DTI prediction method predicts a real-valued score \hat{Y}_{xz} indicating the confidence of the affinity between d_x and t_z . There are four prediction settings according to whether the drug and target involved in the test pair are included in the training set or not [Pahikkala *et al.*, 2015]:

- S1: predict the interaction between $d_x \in D$ and $t_z \in T$
- S2: predict the interaction between $d_x \notin D$ and $t_z \in T$
- S3: predict the interaction between $d_x \in D$ and $t_z \notin T$
- S4: predict the interaction between $d_x \notin D$ and $t_z \notin T$

where $d_x \notin D$ ($t_z \notin T$) is the new drug (target).

2.2 MF for DTI prediction

In DTI prediction, the MF method learns two r -dimensional low-rank latent features (embeddings) $\mathbf{U} \in \mathbb{R}^{n \times r}$ (for drugs) and $\mathbf{V} \in \mathbb{R}^{m \times r}$ (for targets) that approximate the training interaction matrix by minimizing the follow objective:

$$\min_{\mathbf{U}, \mathbf{V}} \mathcal{J} = \mathcal{L}(\hat{\mathbf{Y}}, \mathbf{Y}) + \mathcal{R}(\mathbf{U}, \mathbf{V}) \quad (1)$$

$\mathcal{L}(\hat{\mathbf{Y}}, \mathbf{Y})$ is the loss function, $\hat{\mathbf{Y}} = \sigma(\mathbf{U}\mathbf{V}^\top) \in \mathbb{R}^{n \times m}$ is the predicted interaction matrix, where σ is either the identity function σ_1 for standard MF [Ezzat *et al.*, 2017] or the element-wise logistic function σ_2 for Logistic MF [Liu *et al.*, 2016]. $\mathcal{R}(\mathbf{U}, \mathbf{V})$ concerns the regularization of the latent features and is defined as:

$$\begin{aligned} \mathcal{R}(\mathbf{U}, \mathbf{V}) = & \frac{\lambda_r}{2} (\|\mathbf{U}\|_F^2 + \|\mathbf{V}\|_F^2) \\ & + \frac{\lambda_u}{2} \text{tr}(\mathbf{U}^\top \mathbf{L}^d \mathbf{U}) + \frac{\lambda_v}{2} \text{tr}(\mathbf{V}^\top \mathbf{L}^t \mathbf{V}) \end{aligned} \quad (2)$$

where λ_r , λ_d , λ_t are regularization coefficients, while \mathbf{L}^d and \mathbf{L}^t are the graph Laplacians of the sparse drug and target similarity matrices, respectively. Following the sparsification process in [Liu *et al.*, 2016], we obtain the sparse drug similarity matrix $\hat{\mathbf{S}}^d \in \mathbb{R}^{n \times n}$ by retaining the k -largest similarities in each row of \mathbf{S}^d , i.e. $\hat{S}_{ij}^d = S_{ij}^d$ if $d_j \in \mathcal{N}_{d_i}^k$, where $\mathcal{N}_{d_i}^k$ is k nearest neighbors (most similar drugs) of d_i , and $\hat{S}_{ij}^d = 0$ otherwise. The Laplacian matrix for $\hat{\mathbf{S}}^d$ is defined as $\mathbf{L}^d = \mathbf{\Lambda}^d - \hat{\mathbf{S}}^d + \tilde{\mathbf{\Lambda}}^d - (\hat{\mathbf{S}}^d)^\top$, where $\mathbf{\Lambda}^d$ and $\tilde{\mathbf{\Lambda}}^d$ are two

diagonal matrices with diagonal elements $\Lambda_{ii}^d = \sum_{j=1}^m \hat{S}_{ij}^d$ and $\tilde{\Lambda}_{jj}^d = \sum_{i=1}^n \hat{S}_{ij}^d$, respectively. The sparse target similarity matrix $\hat{\mathbf{S}}^t$ and its graph Laplacian \mathbf{L}^t are computed in the same way. The first term in $\mathcal{R}(\mathbf{U}, \mathbf{V})$ applies Tikhonov regularization that prevents latent features from overfitting to the training data, while the last two terms apply graph regularization, which guarantees their local invariance [Liu *et al.*, 2018], i.e. similar drugs (targets) are likely to have similar latent features.

Given a test drug-target pair (d_x, t_z) , the latent features of d_x and t_z , denoted as $\mathbf{U}_x \in \mathbb{R}^r$ and $\mathbf{V}_z \in \mathbb{R}^r$ respectively, are obtained firstly. If d_x (t_z) is a training drug (target), its latent features are directly extracted from \mathbf{U} (\mathbf{V}), e.g. \mathbf{U}_x is the x -th row of \mathbf{U} . For a new drug (target), we infer its latent features by linearly combining the embeddings of its k -nearest training drugs (targets) using the following equations:

$$\mathbf{U}_x = \frac{1}{\sum_{d_i \in \mathcal{N}_{d_x}^k} s_{xi}^d} \sum_{d_i \in \mathcal{N}_{d_x}^k} \eta^{i'-1} s_{xi}^d \mathbf{U}_i \quad (3)$$

$$\mathbf{V}_z = \frac{1}{\sum_{t_j \in \mathcal{N}_{t_z}^k} s_{zj}^t} \sum_{t_j \in \mathcal{N}_{t_z}^k} \eta^{j'-1} s_{zj}^t \mathbf{V}_j \quad (4)$$

where i' (j') is the rank of d_i (t_j) among $\mathcal{N}_{d_x}^k$, e.g. i' is 2 if d_i is the second nearest neighbor of d_x , $\eta \in [0, 1]$ is the decay coefficient shrinking the weight of further neighbors, and s_{xi}^d (s_{zj}^t) is the similarity between the new drug d_x (target t_z) and the training drug d_i (target t_j). The decay coefficient is an important parameter for nearest neighbors aggregation [Ezzat *et al.*, 2017; Liu *et al.*, 2020], which we use in Eq. (3) and (4) to obtain more reliable latent features for new drugs and targets, in contrast to [Liu *et al.*, 2016]. Then, the MF model outputs its prediction with a specific instantiation of the σ :

$$\hat{Y}_{xz} = \begin{cases} \mathbf{U}_x \mathbf{V}_z^\top, & \text{if } \sigma = \sigma_1 \\ (1 + \exp(-\mathbf{U}_x \mathbf{V}_z^\top))^{-1}, & \text{if } \sigma = \sigma_2 \end{cases} \quad (5)$$

2.3 MFAUPR

The computation of AUPR with linear interpolations on the precision-recall (PR) curve leads to overly-optimistic performance estimation [Davis and Goadrich, 2006]. Therefore, we employ the uninterpolated PR curve to compute AUPR. Given \mathbf{Y} and its predictions $\hat{\mathbf{Y}}$, all predictions are firstly sorted in descending order. Let $R_h = (i_h, j_h)$ be the index tuple of the h -th largest prediction. Based on the rank list R , AUPR is computed as:

$$AUPR(\hat{\mathbf{Y}}, \mathbf{Y}) = \sum_{h=1}^{nm} \text{Prec@}h * \text{InRe@}h \quad (6)$$

where $\text{Prec@}h = \frac{1}{h} \sum_{i=1}^h Y_{R_i}$ is the precision of the first h predictions, $\text{InRe@}h = Y_{R_h} / \psi(\mathbf{Y})$ is the incremental recall from rank $h-1$ to h , and $\psi(\mathbf{Y}) = \sum_i \sum_j Y_{ij}$ denotes the summation of elements in \mathbf{Y} . The AUPR defined in Eq.(6) is also called *Average Precision* [Manning *et al.*, 2009].

AUPR is hard to optimize directly, because it depends on the ranks of the predictions obtained by the non-differentiable

and non-smooth sorting operation. Histogram binning that assigns the predictions into several ordered groups to simulate the ranking process provides a differential substitution for the sorting operation [He *et al.*, 2018; Revaud *et al.*, 2019]. MFAUPR employs the histogram binning strategy to derive the approximate differential AUPR. To divide histogram bins easily, MFAUPR uses the element wise logistic function σ_2 for predictions, i.e. $\hat{Y}_{ij} = (1 + \exp(-\mathbf{U}_i \mathbf{V}_j^\top))^{-1}$, to confine all predictions in the range of (0, 1). The range of predictions is divided into M bins (intervals), and the h -th bin is $\bar{b}_h = [\max(b_h - \Delta, 0), \min(b_h + \Delta, 1)]$, where $\Delta = 1/(M - 1)$ is the bin width and $b_h = 1 - (h - 1)\Delta$ is the center of \bar{b}_h . It should be noted that \bar{b}_1 and \bar{b}_M are half-sized bins.

The soft assignment function that returns the membership degree of a prediction to \bar{b}_h is defined as:

$$\delta(\hat{Y}_{ij}, h) = \max\left(1 - |\hat{Y}_{ij} - b_h|/\Delta, 0\right) \quad (7)$$

where the closer \hat{Y}_{ij} is to b_h , the higher the membership degree of \hat{Y}_{ij} to \bar{b}_h , and vice versa. $\delta(\hat{Y}_{ij}, h)$ is a differentiable function [Revaud *et al.*, 2019] and its derivative w.r.t \hat{Y}_{ij} is:

$$\nabla_{\hat{Y}_{ij}} \delta(\hat{Y}_{ij}, h) = -\frac{1}{\Delta} \text{sign}(\hat{Y}_{ij} - b_h) \mathbb{I}[|\hat{Y}_{ij} - b_h| \leq \Delta] \quad (8)$$

where $\text{sign}(\cdot)$ is the sign function that returns 1 and -1 for positive and negative input values respectively. Furthermore, we define the matrix version of $\delta(\cdot, h)$ and its derivative as: $\delta(\hat{\mathbf{Y}}, h) \in \mathbb{R}^{n \times m}$ with $[\delta(\hat{\mathbf{Y}}, h)]_{ij} = \delta(\hat{Y}_{ij}, h)$ and $\nabla \delta(\hat{\mathbf{Y}}, h) \in \mathbb{R}^{n \times m}$ with $[\nabla \delta(\hat{\mathbf{Y}}, h)]_{ij} = \nabla_{\hat{Y}_{ij}} \delta(\hat{Y}_{ij}, h)$.

Based on the definition of the bin and soft assignment function, the differential approximations of the precision at \bar{b}_h and the increment of recall from \bar{b}_{h-1} to \bar{b}_h are defined as:

$$\text{Prec}'@h = \frac{\sum_{i=1}^h \psi(\delta(\hat{\mathbf{Y}}, i) \odot \mathbf{Y})}{\sum_{i=1}^h \psi(\delta(\hat{\mathbf{Y}}, i))} \quad (9)$$

$$\text{InRe}'@h = \frac{1}{\psi(\mathbf{Y})} \psi(\delta(\hat{\mathbf{Y}}, h) \odot \mathbf{Y}) \quad (10)$$

where \odot is the element-wise product. The differential approximation of AUPR that accumulates the precision and incremental recall of every bins is:

$$\text{AUPR}' = \sum_{h=1}^M \text{Prec}'@h * \text{InRe}'@h \quad (11)$$

Based on Eq. (9)-(11), we obtain the AUPR based loss by ignoring the constant value $\psi(\mathbf{Y})$:

$$\mathcal{L}_{AP} = -\frac{\psi(\delta(\hat{\mathbf{Y}}, h) \odot \mathbf{Y}) \sum_{i=1}^h \psi(\delta(\hat{\mathbf{Y}}, i) \odot \mathbf{Y})}{\sum_{i=1}^h \psi(\delta(\hat{\mathbf{Y}}, i))} \quad (12)$$

Minimizing \mathcal{L}_{AP} is equivalent to maximizing AUPR' . By replacing $\mathcal{L}(\hat{\mathbf{Y}}, \mathbf{Y})$ with \mathcal{L}_{AP} , we define the optimization problem of MFAUPR as:

$$\min_{\mathbf{U}, \mathbf{V}} \mathcal{J}_{AP} = \mathcal{L}_{AP} + \mathcal{R}(\mathbf{U}, \mathbf{V}) \quad (13)$$

Algorithm 1: Training of MFAUPR

input : $\mathbf{Y}, D, T, \mathbf{S}^d, \mathbf{S}^t, \theta, k, \mathcal{C}$

output: $\mathbf{U}, \mathbf{V}, \eta_2, \eta_3, \eta_4$

1 Compute \mathbf{L}^d and \mathbf{L}^t based on sparsified \mathbf{S}^d and \mathbf{S}^t ;

2 Initialize \mathbf{U} and \mathbf{V} randomly;

3 **repeat**

4 $\nabla_{\mathbf{U}} \mathcal{J}_{AP} \leftarrow \nabla_{\mathbf{U}} \mathcal{L}_{AP} + \nabla_{\mathbf{U}} \mathcal{R}(\mathbf{U}, \mathbf{V})$;

5 $\mathbf{U} \leftarrow \mathbf{U} - \theta \nabla_{\mathbf{U}} \mathcal{J}_{AP}$;

6 $\nabla_{\mathbf{V}} \mathcal{J}_{AP} \leftarrow \nabla_{\mathbf{V}} \mathcal{L}_{AP} + \nabla_{\mathbf{V}} \mathcal{R}(\mathbf{U}, \mathbf{V})$;

7 $\mathbf{V} \leftarrow \mathbf{V} - \theta \nabla_{\mathbf{V}} \mathcal{J}_{AP}$;

8 **until convergence**;

9 Choose η_2, η_3, η_4 from \mathcal{C} using Algorithm 2;

Eq. (13) can be solved by alternating optimization [Liu *et al.*, 2016; Ezzat *et al.*, 2017]. In each iteration, \mathbf{U} is firstly updated with fixed \mathbf{V} , and then \mathbf{V} is updated with fixed \mathbf{U} . For the sake of conciseness, we define the following variables: $\psi'_h = \psi(\delta(\hat{\mathbf{Y}}, h))$, $\psi_h = \psi(\delta(\hat{\mathbf{Y}}, h) \odot \mathbf{Y})$, $\Psi_h = \sum_{i=1}^h \psi_i$, $\Psi'_h = \sum_{i=1}^h \psi'_i$, $\mathbf{Z}'_h = \nabla \delta(\hat{\mathbf{Y}}, h) \odot \hat{\mathbf{Y}} \odot (\mathbf{1} - \hat{\mathbf{Y}})$, $\mathbf{Z}_h = \hat{\mathbf{Y}} \odot \mathbf{Z}'_h$. The gradients of \mathcal{L}_{AP} w.r.t \mathbf{U} and \mathbf{V} are:

$$\nabla_{\mathbf{U}} \mathcal{L}_{AP} = \sum_{h=1}^M \frac{\psi_h}{(\Psi'_h)^2} \left(\Psi_h \sum_{i=1}^h \mathbf{Z}'_i \mathbf{V} - \Psi'_h \sum_{i=1}^h \mathbf{Z}_i \mathbf{V} \right) - \frac{\Psi_h}{\Psi'_h} \mathbf{Z}_h \mathbf{V} \quad (14)$$

$$\nabla_{\mathbf{V}} \mathcal{L}_{AP} = \sum_{h=1}^M \frac{\psi_h}{(\Psi'_h)^2} \left(\Psi_h \sum_{i=1}^h \mathbf{Z}'_i{}^\top \mathbf{U} - \Psi'_h \sum_{i=1}^h \mathbf{Z}_i{}^\top \mathbf{U} \right) - \frac{\Psi_h}{\Psi'_h} \mathbf{Z}_h{}^\top \mathbf{U} \quad (15)$$

According to Eq. (2), the gradients of the regularization term w.r.t \mathbf{U} and \mathbf{V} are:

$$\nabla_{\mathbf{U}} \mathcal{R}(\mathbf{U}, \mathbf{V}) = \lambda_r \mathbf{U} + \lambda_u \mathbf{L}^d \mathbf{U} \quad (16)$$

$$\nabla_{\mathbf{V}} \mathcal{R}(\mathbf{U}, \mathbf{V}) = \lambda_r \mathbf{V} + \lambda_u \mathbf{L}^t \mathbf{V} \quad (17)$$

The training process of MFAUPR is shown in Algorithm 1, where θ is the learning rate, k is the number of neighbors to infer latent features, and \mathcal{C} is the set of candidate values for η .

As we mentioned before, η has crucial impact on the quality of the estimated latent features. In MFAUPR, instead of tuning η as a hyper-parameter using grid search, which is time-consuming, the optimal η for each prediction setting (e.g. η_2 is the optimal value for S2) is chosen based on the training set after solving Eq (13), as shown in Algorithm 2. Specifically, given an η from \mathcal{C} , we compute the pseudo latent features of training drugs and targets, which along with \mathbf{U} and \mathbf{V} are used to compute three prediction matrices under three assumed prediction settings (S2, S3 and S4) respectively (line 8, Algorithm 2), e.g. the estimated drug, \mathbf{U}' , and target, \mathbf{V} , latent features are used to make predictions for S2. Then, the AUPR of these prediction matrices are obtained. The above procedure is repeated for all η candidates. For each setting, the η whose prediction matrix achieves the highest AUPR is

the optimal one. In prediction phase, the prediction setting of the test pair is identified, and the corresponding optimal η is used to infer the latent features of the test drug and/or target.

Algorithm 2: Choose Optimal η for Various Settings

input : $\mathbf{Y}, \mathbf{S}^d, \mathbf{S}^t, \mathbf{U}, \mathbf{V}, k, \mathcal{C}$
output: η_2, η_3, η_4
1 $\beta_2, \beta_3, \beta_4 \leftarrow 0, 0, 0$;
2 $\mathbf{U}', \mathbf{V}' \leftarrow \mathbf{0}, \mathbf{0}$; /* pseudo latent features */
3 **for** $\eta \in \mathcal{C}$ **do**
4 **for** $x \leftarrow 1$ **to** n **do**
5 Compute \mathbf{U}'_x according to Eq.(3) with η ;
6 **for** $z \leftarrow 1$ **to** m **do**
7 Compute \mathbf{V}'_z according to Eq.(4) with η ;
8 $\hat{\mathbf{Y}}^2, \hat{\mathbf{Y}}^3, \hat{\mathbf{Y}}^4 \leftarrow$
 $\sigma_2(\mathbf{U}'\mathbf{V}'^\top), \sigma_2(\mathbf{U}\mathbf{V}'^\top), \sigma_2(\mathbf{U}'\mathbf{V}^\top)$;
9 **for** $i \leftarrow 2$ **to** 4 **do**
10 $\beta = \text{AUPR}(\hat{\mathbf{Y}}^i, \mathbf{Y})$;
11 **if** $\beta > \beta_i$ **then**
12 $\beta_i, \eta_i \leftarrow \beta, \eta$;

The computational cost of MFAUPR depends mainly on the calculation of the gradients of the objective function in each iteration of the optimization. The complexities of computing gradients of \mathcal{L}_{AP} , $\nabla_{\mathbf{U}}\mathcal{R}(\mathbf{U}, \mathbf{V})$ and $\nabla_{\mathbf{V}}\mathcal{R}(\mathbf{U}, \mathbf{V})$ are $O(Mrnm)$, $O(rn^2)$ and $O(rm^2)$, respectively. Thus, the overall complexity of MFAUPR is $O(Mr * \max\{n^2, m^2\})$.

2.4 MFAUC

Given \mathbf{Y} and its predictions $\hat{\mathbf{Y}}$, AUC, which counts the proportion of tuples where the interacting pair has higher prediction than the non-interacting one, is defined as:

$$\text{AUC}(\hat{\mathbf{Y}}, \mathbf{Y}) = \frac{1}{|W|} \sum_{(ij, hl) \in W} \mathbb{I}[\hat{Y}_{ij} > \hat{Y}_{hl}] \quad (18)$$

where $\mathbb{I}[\pi]$ is the indicator function which returns 1 when π hold, and 0 otherwise. $W_1 = \{(i, j) | Y_{ij} = 1\}$ is the set of all interacting drug-target pairs, $W_0 = \{(i, j) | Y_{ij} = 0\}$ is the set of all non-interacting pairs, and $W = \{(i, j), (h, l) | (i, j) \in W_1, (h, l) \in W_0\}$ is the Cartesian product of W_1 and W_0 . For simplicity, we use (ij, hl) to denote $((i, j), (h, l))$ in sequel.

The maximization of the AUC metric is equivalent to the minimization of the following loss:

$$\mathcal{L}'_{AUC} = \sum_{(ij, hl) \in W} \mathbb{I}[\hat{Y}_{ij} \leq \hat{Y}_{hl}] \quad (19)$$

Although the discontinuous of indicator function would make the minimization of \mathcal{L}'_{AUC} render to the NP hard problem, we can derive a convex AUC loss which is consistency with Eq. (19) by replacing the indicator function with a convex surrogate function $\phi(\cdot)$ [Gao and Zhou, 2015; Gultekin *et al.*, 2020]:

$$\mathcal{L}_{AUC} = \sum_{(ij, hl) \in W} \phi(\zeta_{ijhl}) \quad (20)$$

where $\zeta_{ijhl} = \hat{Y}_{ij} - \hat{Y}_{hl}$. In MFAUC, ϕ is defined as the logistic loss function, i.e. $\phi(x) = \log(1 + \exp(-x))$, and its derivative is $\phi'(x) = -(1 + \exp(x))^{-1}$. Besides, the prediction of MFAUC is defined as $\hat{\mathbf{Y}} = \mathbf{U}\mathbf{V}^\top$. By replacing $\mathcal{L}(\hat{\mathbf{Y}}, \mathbf{Y})$ with \mathcal{L}_{AUC} defined in Eq.(1), we obtain the optimization problem of MFAUC:

$$\min_{\mathbf{U}, \mathbf{V}} \mathcal{J}_{AUC} = \mathcal{L}_{AUC} + \mathcal{R}(\mathbf{U}, \mathbf{V}) \quad (21)$$

Similar to MFAUPR, we solve the Eq. (21) by updating \mathbf{U} and \mathbf{V} alternatively. The gradient of \mathcal{L}_{AUC} w.r.t \mathbf{U}_i is

$$\nabla_{\mathbf{U}_i} \mathcal{L}_{AUC} = \sum_{(ij, hl) \in W} \phi'(\zeta_{ijhl}) \mathbf{V}_j - \sum_{(hl, ij) \in W} \phi'(\zeta_{hlij}) \mathbf{V}_j \quad (22)$$

Because $|W|$ is quadratic to nm , the computational complexity of calculating $\nabla_{\mathbf{U}_i} \mathcal{L}_{AUC}$ is $O(n^2m)$ which is costly even for hundreds of drugs and targets. To speed up the computation, we approximate $\nabla_{\mathbf{U}_i} \mathcal{L}_{AUC}$ by using a nm sized set W' sampled from W to reduce the complexity to $O(m)$:

$$\nabla_{\mathbf{U}_i} \mathcal{L}_{AUC} \approx \sum_{(ij, hl) \in W'} \phi'(\zeta_{ijhl}) \mathbf{V}_j - \sum_{(hl, ij) \in W'} \phi'(\zeta_{hlij}) \mathbf{V}_j \quad (23)$$

Based on Eq.(23), the gradient of \mathcal{L}_{AUC} w.r.t \mathbf{U} is defined as:

$$\nabla_{\mathbf{U}} \mathcal{L}_{AUC} = \left[(\nabla_{\mathbf{U}_1} \mathcal{L}_{AUC})^\top, \dots, (\nabla_{\mathbf{U}_n} \mathcal{L}_{AUC})^\top \right]^\top \quad (24)$$

Similarly, the gradient of \mathcal{L}_{AUC} w.r.t \mathbf{V} is

$$\nabla_{\mathbf{V}} \mathcal{L}_{AUC} = \left[(\nabla_{\mathbf{V}_1} \mathcal{L}_{AUC})^\top, \dots, (\nabla_{\mathbf{V}_m} \mathcal{L}_{AUC})^\top \right]^\top \quad (25)$$

$$\nabla_{\mathbf{V}_j} \mathcal{L}_{AUC} \approx \sum_{(ij, hl) \in W'} \phi'(\zeta_{ijhl}) \mathbf{U}_i - \sum_{(hl, ij) \in W'} \phi'(\zeta_{hlij}) \mathbf{U}_i \quad (26)$$

MFAUC employs the AdaGrad algorithm [Duchi *et al.*, 2011] that adaptively chooses the update step based on previous gradients to diminish the influence of sampling on computing gradients of \mathcal{L}_{AUC} . The training of MFAUC is shown in Algorithm 3, where $\circ a$ denotes the element wise exponentiation with the exponent being a . Besides, in the η selection procedure, predictions of MFAUC are defined as $\hat{\mathbf{Y}}^2 = \mathbf{U}'\mathbf{V}^\top$, $\hat{\mathbf{Y}}^3 = \mathbf{U}\mathbf{V}'^\top$, $\hat{\mathbf{Y}}^4 = \mathbf{U}'\mathbf{V}'^\top$ (line 8, Algorithm 2) and the η with best AUC is the optimal value.

In MFAUC, the complexity of calculating gradients of \mathcal{L}_{AUC} using the sampled set W' is $O(rnm)$, and other steps have the same complexity with MFAUPR. Thus, the complexity of MFAUC is $O(r * \max\{n^2, m^2\})$.

3 Experiments

3.1 Experimental Setup

Four benchmark DTI datasets constructed in 2007 of which each corresponds to a target protein family, namely Nuclear Receptors (NR), Ion Channel (IC), G-protein coupled receptors (GPCR), Enzyme (E) [Yamanishi *et al.*, 2008] are used. In these datasets, similarities between drugs are measured

Algorithm 3: Training of MFAUC

input : $Y, D, T, S^d, S^t, \theta, k, \mathcal{C}$
output: $U, V, \eta_2, \eta_3, \eta_4$

- 1 Compute L^d and L^t based on sparsified S^d and S^t ;
- 2 Initialize U and V randomly;
- 3 $G, H \leftarrow \mathbf{0}, \mathbf{0}$; /* accumulated gradients */
- 4 **repeat**
- 5 $\nabla_U \mathcal{J}_{AUC} \leftarrow \nabla_U \mathcal{L}_{AUC} + \nabla_U \mathcal{R}(U, V)$;
- 6 $G \leftarrow G + (\nabla_U \mathcal{J}_{AUC})^{\circ 2}$;
- 7 $U \leftarrow U - \theta \nabla_U \mathcal{J}_{AUC} \odot G^{\circ -\frac{1}{2}}$;
- 8 $\nabla_V \mathcal{J}_{AUC} \leftarrow \nabla_V \mathcal{L}_{AUC} + \nabla_V \mathcal{R}(U, V)$;
- 9 $H \leftarrow H + (\nabla_V \mathcal{J}_{AUC})^{\circ 2}$;
- 10 $V \leftarrow V - \theta \nabla_V \mathcal{J}_{AUC} \odot H^{\circ -\frac{1}{2}}$;
- 11 **until** convergence;
- 12 Choose η_2, η_3, η_4 from \mathcal{C} using Algorithm 2;

by using the SIMCOMP algorithm on compound chemical structure [Hattori *et al.*, 2003] and target similarities are assessed by normalized Smith–Waterman score for protein sequences [Smith and Waterman, 1981]. Because the interactions in these datasets were found 13 years ago, we update them by adding newly discovered interactions between drugs and targets in these datasets recorded in the last version of KEGG¹, DrugBank² and ChEMBL³ databases. The four updated datasets are shown in Table 1.

Table 1: Datasets

Dataset	#Drugs	#Targets	#Interactions
NR	54	26	166
GPCR	223	95	1096
IC	210	204	2331
E	445	664	4256

The two proposed methods are compared with six DTI prediction approaches, including **NRLMF** [Liu *et al.*, 2016]: MF optimizing logistic loss, **GRMF** [Ezzat *et al.*, 2017]: MF optimizing square loss with an interaction estimation pre-processing, **BRDTI** [Peska *et al.*, 2017]: Bayesian ranking approach optimizing drug-based ranking loss, **KronSVM** [Airola and Pahikkala, 2018]: Kronecker product kernel method optimizing square hinge loss, **WkNNRI** [Liu *et al.*, 2020]: neighborhood based method and **EBiCTR** [Pliakos and Vens, 2020]: ensemble of bi-clustering trees. The parameters of the comparing methods are set or chosen based on the suggestions in respective articles. For MFAUPR and MFAUC, $k=5, \theta=0.1, \mathcal{C}=\{0.1, 0.2, \dots, 1.0\}$, the number of iterations is 100, r is chosen from $\{50, 100\}$, λ_d, λ_t and λ_r are chosen from $\{2^{-4}, 2^{-2}, 2^0, 2^2\}$. M in MFAUPR is chosen from $\{11, 16, 21, 26, 31\}$.

Following [Pahikkala *et al.*, 2015], four types of cross validation (CV) are conducted to examine the methods in four prediction settings, respectively. In S1, the 10-fold CV on

¹<https://www.genome.jp/kegg/>

²<https://go.drugbank.com/>

³<https://www.ebi.ac.uk/chembl/>

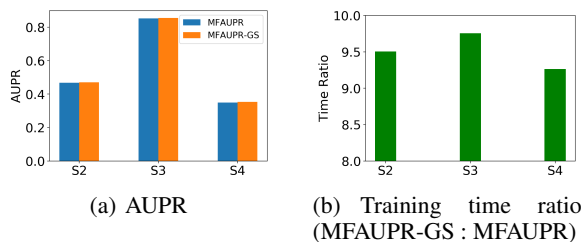


Figure 1: Comparison of MFAUPR and MFAUPR-GS on IC dataset

pairs is used, where one fold of pairs are removed for testing. In S2 (S3), the 10-fold CV on drugs (targets) is applied, where one drug (target) fold along with their corresponding rows (columns) in Y are separated for testing. The 3×3 -fold block-wise CV which splits a drug fold and target fold along with the interactions between them for testing and uses interactions between remaining drugs and targets for training, is applied to S4. All CVs are repeated two times, and the average results are reported. Furthermore, AUPR and AUC defined in Eq. (6) and (18) are used as evaluation measures.

3.2 Experimental Results

The results in terms of AUPR and AUC are shown in Table 2 and 3 respectively, where the last row lists the average ranks across all settings, and \bullet (\star) indicates the corresponding method is significantly different from MFAUPR (MFAUC) according to Wilcoxon signed-rank test at 5% level on the results of all settings. The results of WkNNRI and EBiCTR in S1 are blank because they cannot deal with S1.

In terms of AUPR, MFAUPR is the best method and significantly outperforms all six competitors, followed by MFAUC which is significantly better than four comparing methods. In addition, MFAUPR is the top method in S3 and S4, and the second best method in S1 and S2. Although MFAUC and WkNNRI perform best in S1 and S2 respectively, they are inferior to MFAUPR in other settings. In terms of AUC, MFAUC is the most effective approach for all settings, achieving significant superiority to MFAUPR and all competitors except for NRLMF which is the second best method. MFAUPR comes next and its difference with NRLMF is not significant. BRDTI which optimizes drug-based ranking loss is the runner-up in S2, where interactions for new drugs are predicted, but performs worse in other settings. Overall, the MFAUPR and MFAUC not only achieve the most outstanding performance in terms of the corresponding metric they optimize, but also perform well in terms of the other metric.

To examine the effectiveness of the proposed optimal η selection strategy, we compare the results and the total training time of MFAUPR and a variant of MFAUPR (denoted as MFAUPR-GS) that turns η via grid search, i.e. training 10 models for 10 η candidates respectively and choosing the one that achieves the best AUPR on the test set. As shown in Figure 1, MFAUPR achieves similar performance with MFAUPR-GS with more than 9 times speed-up.

Figure 2 shows the convergence curves of MFAUPR and MFAUC on IC dataset in S1. The values of the objective

Setting	Dataset	NRLMF	GRMF	BRDTI	KronSVM	WKNNRI	EBiCTR	MFAUPR	MFAUC
S1	NR	0.648(1)	0.623(4)	0.574(6)	0.581(5)	-	-	0.645(2)	0.625(3)
	GPCR	0.851(3)	0.841(4)	0.728(6)	0.788(5)	-	-	0.859(2)	0.867(1)
	IC	0.929(3)	0.92(4)	0.747(6)	0.86(5)	-	-	0.937(1)	0.934(2)
	E	0.833(2)	0.81(4)	0.711(6)	0.738(5)	-	-	0.827(3)	0.839(1)
<i>AveRank</i>		2.25	4	6	5	-	-	2	1.75
S2	NR	0.546(3.5)	0.537(6)	0.545(5)	0.503(8)	0.566(2)	0.515(7)	0.567(1)	0.546(3.5)
	GPCR	0.473(7)	0.479(5)	0.489(4)	0.42(8)	0.513(1)	0.476(6)	0.503(2)	0.498(3)
	IC	0.466(5)	0.459(6)	0.468(3.5)	0.413(8)	0.472(1)	0.457(7)	0.468(3.5)	0.469(2)
	E	0.377(5)	0.382(4)	0.352(6)	0.275(8)	0.393(2)	0.341(7)	0.395(1)	0.391(3)
<i>AveRank</i>		5.13	5.25	4.63	8	1.5	6.75	1.88	2.88
S3	NR	0.501(4)	0.484(6)	0.46(7)	0.502(3)	0.527(2)	0.453(8)	0.55(1)	0.485(5)
	GPCR	0.683(7)	0.689(6)	0.547(8)	0.755(2)	0.742(4)	0.69(5)	0.754(3)	0.762(1)
	IC	0.857(1)	0.853(3)	0.778(8)	0.849(5)	0.846(6)	0.836(7)	0.853(3)	0.853(3)
	E	0.696(1)	0.682(5)	0.666(6)	0.644(7)	0.685(4)	0.64(8)	0.692(2)	0.688(3)
<i>AveRank</i>		3.25	5	7.25	4.25	4	7	2.25	3
S4	NR	0.273(6)	0.277(5)	0.309(1)	0.253(8)	0.283(4)	0.293(2)	0.287(3)	0.262(7)
	GPCR	0.306(4)	0.302(6)	0.291(7)	0.304(5)	0.332(3)	0.28(8)	0.344(2)	0.356(1)
	IC	0.343(4)	0.337(7)	0.348(3)	0.341(6)	0.342(5)	0.32(8)	0.35(2)	0.352(1)
	E	0.223(2)	0.218(4)	0.212(5)	0.109(8)	0.223(2)	0.171(7)	0.223(2)	0.201(6)
<i>AveRank</i>		4	5.5	4	6.75	3.5	6.25	2.25	3.75
<i>Summary</i>		3.66●	4.94●★	5.47●★	6●★	3●	6.88●★	2.09	2.84

Table 2: AUPR Results

Setting	Dataset	NRLMF	GRMF	BRDTI	KronSVM	WKNNRI	EBiCTR	MFAUPR	MFAUC
S1	NR	0.875(2)	0.871(3)	0.853(5)	0.828(6)	-	-	0.884(1)	0.87(4)
	GPCR	0.97(3)	0.968(4)	0.958(5)	0.956(6)	-	-	0.975(1)	0.974(2)
	IC	0.987(1.5)	0.982(3.5)	0.944(6)	0.963(5)	-	-	0.982(3.5)	0.987(1.5)
	E	0.977(2)	0.966(5)	0.968(3.5)	0.948(6)	-	-	0.968(3.5)	0.978(1)
<i>AveRank</i>		2.13	3.88	4.88	5.75	-	-	2.25	2.13
S2	NR	0.817(5)	0.812(6)	0.83(1)	0.794(8)	0.823(2)	0.801(7)	0.819(4)	0.821(3)
	GPCR	0.9(3)	0.897(5.5)	0.898(4)	0.801(8)	0.897(5.5)	0.895(7)	0.911(2)	0.919(1)
	IC	0.813(2)	0.809(5)	0.81(4)	0.791(7)	0.806(6)	0.815(1)	0.785(8)	0.812(3)
	E	0.863(4)	0.865(3)	0.877(2)	0.749(8)	0.843(7)	0.856(5)	0.855(6)	0.89(1)
<i>AveRank</i>		3.5	4.88	2.75	7.75	5.13	5	5	2
S3	NR	0.807(3)	0.793(5)	0.768(7)	0.786(6)	0.803(4)	0.764(8)	0.808(2)	0.81(1)
	GPCR	0.954(3)	0.943(5)	0.925(8)	0.933(6)	0.947(4)	0.931(7)	0.955(2)	0.961(1)
	IC	0.959(3)	0.957(4)	0.951(6)	0.943(8)	0.948(7)	0.953(5)	0.961(2)	0.963(1)
	E	0.936(1)	0.912(4.5)	0.901(7)	0.896(8)	0.902(6)	0.922(3)	0.912(4.5)	0.929(2)
<i>AveRank</i>		2.5	4.63	7	7	5.25	5.75	2.63	1.25
S4	NR	0.696(2)	0.667(4)	0.723(1)	0.644(7)	0.663(6)	0.618(8)	0.689(3)	0.664(5)
	GPCR	0.864(3)	0.855(5)	0.849(7)	0.789(8)	0.86(4)	0.851(6)	0.869(2)	0.886(1)
	IC	0.754(4)	0.76(1)	0.739(7)	0.742(5)	0.759(2)	0.74(6)	0.737(8)	0.756(3)
	E	0.791(6)	0.798(5)	0.772(7)	0.648(8)	0.804(2)	0.8(4)	0.803(3)	0.818(1)
<i>AveRank</i>		3.75	3.75	5.5	7	3.5	6	4	2.5
<i>Summary</i>		2.97	4.28★	5.03★	6.88●★	4.63★	6.06★	3.47★	1.97

Table 3: AUC Results

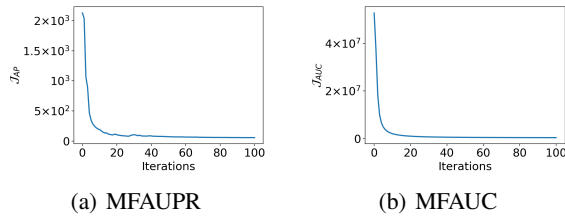


Figure 2: Convergence curves on IC dataset in S1

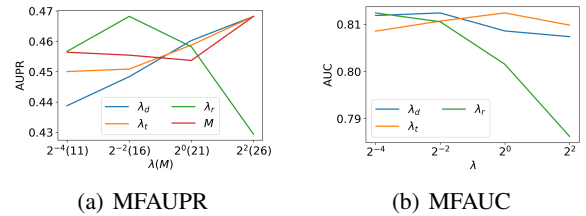


Figure 3: Results with various parameter values on IC dataset in S2

functions drop sharply in the first 10 iterations and then gradually decrease to a stationary state, which demonstrates the convergence of the proposed methods.

The results of MFAUPR and MFAUC with various parameters settings on IC dataset in S2 are shown in Figure 3. With respect to the regularization coefficients, the optimal value of λ_d and λ_t that relate to graph regularization is usually higher

than the best option of λ_r which is in charge of Tikhonov regularization. With respect to the number of bins (M), a larger value provides a more fine grain division for predictions, leading to better performance.

4 Conclusion

This paper presented two graph regularized MF approaches for DTI prediction that optimize AUPR and AUC respectively. Empirical studies on updated benchmark datasets verify the superiority of the proposed methods compared to the state-of-the-art. In the future, we plan to extend our methods to exploit multiple drug and target similarities derived from diverse aspects.

References

- [Airola and Pahikkala, 2018] Antti Airola and Tapio Pahikkala. Fast kronecker product kernel methods via generalized vec trick. *IEEE Transactions on Neural Networks and Learning Systems*, 29(8):3374–3387, 2018.
- [Chen *et al.*, 2018] Ruolan Chen, Xiangrong Liu, Shuting Jin, Jiawei Lin, and Juan Liu. Machine learning for drug-target interaction prediction. *Molecules*, 23(9):2208, 2018.
- [Davis and Goadrich, 2006] Jesse Davis and Mark Goadrich. The relationship between Precision-Recall and ROC curves. In *ICML*, pages 233–240, 2006.
- [Dhanjal *et al.*, 2015] Charanpal Dhanjal, Romaric Gaudel, and Stephan Clemencon. AUC optimisation and collaborative filtering. *arXiv*, 2015.
- [Duchi *et al.*, 2011] John Duchi, Elad Hazan, and Yoram Singer. Adaptive subgradient methods for online learning and stochastic optimization. *Journal of Machine Learning Research*, 12:2121–2159, 2011.
- [Ezzat *et al.*, 2017] Ali Ezzat, Peilin Zhao, Min Wu, Xiao Li Li, and Chee Keong Kwoh. Drug-target interaction prediction with graph regularized matrix factorization. *IEEE/ACM Transactions on Computational Biology and Bioinformatics*, 14(3):646–656, 2017.
- [Ezzat *et al.*, 2018] Ali Ezzat, Min Wu, Xiao Li Li, and Chee Keong Kwoh. Computational prediction of drug-target interactions using chemogenomic approaches: an empirical survey. *Briefings in Bioinformatics*, 20(4):1337–1357, 2018.
- [Gao and Zhou, 2015] Wei Gao and Zhi Hua Zhou. On the consistency of AUC pairwise optimization. In *IJCAI*, pages 939–945, 2015.
- [Gao *et al.*, 2018] Kyle Yingkai Gao, Achille Fokoue, Heng Luo, Arun Iyengar, Sanjoy Dey, and Ping Zhang. Interpretable drug target prediction using deep neural representation. In *IJCAI*, pages 3371–3377, 2018.
- [Golokov *et al.*, 2020] Vladimir Golokov, Alexander Becker, Daniel T. Plopp, Daniel Čuturilo, Neda Davoudi, Jeffrey Mendenhall, Rocco Moretti, Jens Meiler, and Daniel Creemers. Deep learning for virtual screening: Five reasons to use ROC cost functions. *arXiv*, 2020.
- [Gultekin *et al.*, 2020] San Gultekin, Avishek Saha, Adwait Ratnaparkhi, and John Paisley. MBA: Mini-batch AUC optimization. *IEEE Transactions on Neural Networks and Learning Systems*, 31(12):5561–5574, 2020.
- [Hattori *et al.*, 2003] Masahiro Hattori, Yasushi Okuno, Susumu Goto, and Minoru Kanehisa. Development of a chemical structure comparison method for integrated analysis of chemical and genomic information in the metabolic pathways. *Journal of the American Chemical Society*, 125(39):11853–11865, 2003.
- [He *et al.*, 2018] Kun He, Fatih Cakir, Sarah Adel Bargal, and Stan Sclaroff. Hashing as tie-aware learning to rank. In *CVPR*, pages 4023–4032, 2018.
- [Liu *et al.*, 2016] Yong Liu, Min Wu, Chunyan Miao, Peilin Zhao, and Xiao Li Li. Neighborhood regularized logistic matrix factorization for drug-target interaction prediction. *PLoS Computational Biology*, 12(2), 2016.
- [Liu *et al.*, 2018] Jin Xing Liu, Dong Wang, Ying Lian Gao, Chun Hou Zheng, Yong Xu, and Jiguo Yu. Regularized non-negative matrix factorization for identifying differentially expressed genes and clustering samples: A survey. *IEEE/ACM Transactions on Computational Biology and Bioinformatics*, 15(3):974–987, 2018.
- [Liu *et al.*, 2020] Bin Liu, Konstantinos Pliakos, Celine Vens, and Grigorios Tsoumakas. Drug-target interaction prediction via an ensemble of weighted nearest neighbors with interaction recovery. *ArXiv*, 2020.
- [Manning *et al.*, 2009] Christopher D. Manning, Prabhakar Raghavan, and Hinrich Schütze. *An introduction to information retrieval*. Cambridge University Press, 2009.
- [Pahikkala *et al.*, 2015] Tapio Pahikkala, Antti Airola, Sami Pietilä, Sushil Shakyawar, Agnieszka Sz wajda, Jing Tang, and Tero Aittokallio. Toward more realistic drug-target interaction predictions. *Briefings in Bioinformatics*, 16(2):325–337, 2015.
- [Peska *et al.*, 2017] Ladislav Peska, Krisztian Buza, and Júlia Koller. Drug-target interaction prediction: A Bayesian ranking approach. *Computer Methods and Programs in Biomedicine*, 152:15–21, 2017.
- [Pliakos and Vens, 2020] Konstantinos Pliakos and Celine Vens. Drug-target interaction prediction with tree-ensemble learning and output space reconstruction. *BMC Bioinformatics*, 21(1):1V, 2020.
- [Revaud *et al.*, 2019] Jerome Revaud, Jon Almazan, Rafael Rezende, and Cesar De Souza. Learning with average precision: Training image retrieval with a listwise loss. In *ICCV*, pages 5106–5115, 2019.
- [Schrynemackers *et al.*, 2013] Marie Schrynemackers, Robert Küffner, and Pierre Geurts. On protocols and measures for the validation of supervised methods for the inference of biological networks. *Frontiers in Genetics*, 4, 2013.
- [Shi *et al.*, 2012] Yue Shi, Alexandros Karatzoglou, Linas Baltrunas, Martha Larson, Alan Hanjalic, and Nuria Oliver. TFMAP: Optimizing MAP for top-n context-aware recommendation. In *SIGIR*, pages 155–164, 2012.
- [Smith and Waterman, 1981] T. F. Smith and M. S. Waterman. Identification of common molecular subsequences. *Journal of Molecular Biology*, 147(1):195–197, 1981.

[Yamanishi *et al.*, 2008] Yoshihiro Yamanishi, Michihiro Araki, Alex Gutteridge, Wataru Honda, and Minoru Kanehisa. Prediction of drug-target interaction networks from the integration of chemical and genomic spaces. *Bioinformatics*, 24(13), 2008.

[Zheng *et al.*, 2013] Xiaodong Zheng, Hao Ding, Hiroshi Mamitsuka, and Shanfeng Zhu. Collaborative matrix factorization with multiple similarities for predicting drug-Target interactions. In *KDD*, pages 1025–1033, 2013.